

Boron–Nitrogen Coupling in a Ruthenium-rich Ruthenaborane Cluster: Synthesis, and Molecular and Electronic Structures of $[\text{Ru}_4\text{H}(\text{CO})_{12}\text{BH}(\mu\text{-NCHMe})]^\dagger$

Jane R. Galsworthy,^a Catherine E. Housecroft,^{*,a,b} James S. Humphrey,^a Xuejing Song,^a Andrew J. Edwards^c and Arnold L. Rheingold^{*,c}

^a University Chemical Laboratory, Lensfield Road, Cambridge CB2 1EW, UK

^b Institut für Anorganische Chemie, Universität Basel, Spitalstrasse 51, CH-4056 Basel, Switzerland

^c Department of Chemistry, University of Delaware, Newark, DE 19716, USA

The photolysis of $[\text{Ru}_3(\text{CO})_9\text{BH}_5]$ in acetonitrile in the presence of $[\text{M}(\text{CO})_6]$ ($\text{M} = \text{Cr}, \text{Mo}$ or W), with or without Me_3NO , leads to the formation of $[\text{Ru}_4\text{H}(\text{CO})_{12}\text{BH}(\mu\text{-NCHMe})]$ **1** which is a butterfly cluster containing a semi-interstitial boron atom. The crystal structure of **1** has been determined: monoclinic, space group $C2/c$, $a = 37.642(8)$, $b = 9.340(2)$, $c = 13.923(3)$ Å, $\beta = 111.19(2)^\circ$, $Z = 8$, $R = 0.0278$, $R' = 0.0390$. The formation of **1** represents an example of coupling between a nitrogen atom and a boron atom in a metal-rich metallaborane cluster, and is of interest because of the cluster expansion which accompanies the B–N bond formation. The bonding in compound **1** has been investigated by use of the Fenske–Hall approach. These quantum chemical results are consistent with a picture of localized bonding in the region of the B–N–Ru bridge, a conclusion that is also reached by a consideration of the requirements of the cluster valence electron count of 62.

The area of metal-rich metallaborane (defined here as B–H containing) and metallaboride (defined here as not possessing B–H interactions) clusters is an expanding one.^{1–5} Whilst the geometrical environments of the boron atom in homo- or hetero-metallic M_nB cages continue to show intriguing variations, the reactivity of the boron atom with respect to small organic molecules within these environments has yet to be fully explored. Clearly, once the boron atom is completely encapsulated within a metal cage, it, like the carbide before it,⁶ will tend to show a greatly reduced potential for reactivity. On the other hand, in the semi-interstitial state (*e.g.* in a butterfly M_4B skeleton) or in the more exposed environment of the tetrahedral M_3B core, the boron atom is potentially a site for some interesting reactions. This has been elegantly shown for $[\text{Os}_3\text{H}_3(\text{CO})_9\text{B}(\text{CO})]$ and related compounds by Shore and co-workers.^{7–11} In our own work, we have shown that boron–carbon coupling occurs during the reactions of $[\text{Ru}_4\text{H}(\text{CO})_{12}\text{BH}_2]$ with $\text{PhC}\equiv\text{CPh}$ ^{12,13} and $\text{PhC}\equiv\text{CMe}$,¹⁴ or $[\text{Ru}_3\text{WH}(\eta^5\text{-C}_5\text{H}_5)(\text{CO})_{11}\text{BH}]$ with $\text{PhC}\equiv\text{CPh}$.¹³ An accompanying reaction is the cyclodimerization of the alkyne to give a substituted azulene.¹⁴ In this paper, we report an example of boron–nitrogen coupling which is concomitant with the expansion of an Ru_3B - to an Ru_4B -framework in the presence of a labile MeCN ligand.

Experimental

General.—Fourier-transform NMR spectra were recorded on a Bruker WM 250 or AM 400 spectrometer. Proton NMR shifts are reported with respect to δ 0 for SiMe_4 ; ¹¹B NMR with respect to δ 0 for $\text{BF}_3\cdot\text{OEt}_2$. All downfield chemical shifts are positive. Infrared spectra were recorded on a Perkin-Elmer FT 1710 spectrophotometer. Fast atom bombardment (FAB) mass spectra were recorded on Kratos instruments using 3-nitrobenzyl alcohol as the matrix.

Reactions were carried out under argon by using standard Schlenk techniques. Solvents were dried over suitable reagents and freshly distilled under N_2 before use. Separations were carried out by thin-layer plate chromatography with Kieselgel 60-PF-254 (Merck). The compounds $[\text{M}(\text{CO})_6]$ ($\text{M} = \text{Cr}, \text{Mo}$ or W) were used as received (Aldrich). The compound $[\text{Ru}_3(\text{CO})_9\text{BH}_5]$ was prepared as previously described.¹⁵ The reagent Me_3NO (Aldrich) was purified before use. Photolyses were carried out by using a mercury high-pressure lamp (Aldrich).

Preparation of $[\text{Ru}_4\text{H}(\text{CO})_{12}\text{BH}(\mu\text{-NCHMe})]$ **1.**—In a typical reaction, Me_3NO (40 mg, 0.53 mmol) was dissolved in MeCN (2 cm³) and the solution added to $[\text{Mo}(\text{CO})_6]$ (79 mg, 0.3 mmol) previously dissolved in MeCN (2 cm³). To this was added $[\text{Ru}_3(\text{CO})_9\text{BH}_5]$ (57 mg, 0.1 mmol). An immediate colour change from yellow to orange was observed. The volume of solvent was reduced to 2 cm³ and the sample transferred to a quartz photolysis tube. A dark red solution was formed after photolysis for 16 h and the products were separated by TLC. The first fraction was unreacted $[\text{Ru}_3(\text{CO})_9\text{BH}_5]$ ¹⁵ and the second and third fractions were yellow and identified as $[\text{Ru}_4\text{H}(\text{CO})_{12}\text{BH}_2]$ ^{16,17} and $[\text{Ru}_4\text{H}_4(\text{CO})_{12}]$.¹⁸ The fourth fraction was red $[\text{Ru}_4\text{H}_2(\text{CO})_{13}]$.¹⁸ The next band was orange $[\text{Ru}_4\text{H}(\text{CO})_{12}\text{BH}(\mu\text{-NCHMe})]$ **1**. The brown baseline contained insoluble, unidentified material. The same results were obtained if $[\text{Mo}(\text{CO})_6]$ was replaced by $[\text{Cr}(\text{CO})_6]$ or $[\text{W}(\text{CO})_6]$. Yields of **1** varied from 10 to 30% based on conversion from $[\text{Ru}_3(\text{CO})_9\text{BH}_5]$. A second isomer of **1**, **1a**, was further separated by re-separation eluting with hexane.

The reaction may be carried out in the absence of Me_3NO . In this case, $[\text{M}(\text{CO})_{6-x}(\text{MeCN})_x]$ ($\text{M} = \text{Mo}$ or W , $x = 1$ or 2) is first prepared by photolysing $[\text{M}(\text{CO})_6]$ in MeCN, and this solution is added to $[\text{Ru}_3(\text{CO})_9\text{BH}_5]$. The scale of reaction and work-up procedure are the same as described above. The yield of **1** is $\approx 10\%$.

Compound **1**. 400 MHz ¹H NMR (CDCl_3 , 298 K) δ +8.8 (1 H, q, J_{HH} 5.0), +2.3 (3 H, d, J_{HH} 4.8 Hz), –8.0 (br), –20.44 (s); 128 MHz ¹¹B NMR (CDCl_3 , 298 K) δ +77.3 (br);

[†] Supplementary data available: see Instructions for Authors, *J. Chem. Soc., Dalton Trans.*, 1994, Issue 1, pp. xxiii–xxviii.

Table 1 Crystal data for compound **1**

Formula	C ₁₄ H ₆ BNO ₁₂ Ru ₄
<i>M</i>	795.3
Space group	C2/c
<i>a</i> /Å	37.642(8)
<i>b</i> /Å	9.340(2)
<i>c</i> /Å	13.923(3)
β/°	111.19(2)
<i>U</i> /Å ³	4564.3(15)
<i>Z</i>	8
<i>F</i> (000)	2992
<i>T</i> /°C	296
λ(Mo-Kα)/Å	0.710 73
<i>D</i> _c /g Å ⁻³	2.315
μ/cm ⁻¹	26.54
Crystal colour, size/mm	Orange, 0.30 × 0.38 × 0.50
2θ _{max} /°	54
Reflections collected	5498
Independent reflections	4970
Observed reflections	4079 (4σ _{F_o})
<i>R</i> , <i>R</i> '	0.0278, 0.0390
Goodness of fit	1.00
Δρ/e Å ⁻³	0.48
Min., max. transmission	0.3627, 0.5758

$$R = \Sigma \Delta / \Sigma (F_o); R' = \Sigma (\Delta w^3) / (F_o w^3); \Delta = |F_o - F_c|; w^{-1} = \sigma^2(F_o) + 0.0008 F_o^2.$$

IR (CH₂Cl₂, cm⁻¹) ν_{CO} 2098w, 2068s, 2050vs, 2040 (sh), 2011m, 2000w (sh); FAB-mass spectrum *m/z* 794 (*P*⁺) with 11 CO losses (calc. for ¹²C₁₄¹H₆¹¹B₁¹⁴N₁¹⁶O₁₂¹⁰¹Ru₄ 795).

Compound **1a**. 400 MHz ¹H NMR (CDCl₃, 298 K) δ +8.8 (1 H, q, *J*_{HH} 5.0), +2.5 (3 H, d, *J*_{HH} 5.0 Hz), -7.5 (br), -20.56 (s); 128 MHz ¹¹B NMR (CDCl₃, 298 K) δ +77.3 (br); IR (CH₂Cl₂, cm⁻¹) ν_{CO} 2098w, 2068s, 2050vs, 2011m, 1995w (sh); FAB-mass spectrum *m/z* 770 (*P*⁺ - CO) with eight CO losses (calc. for ¹²C₁₄¹H₆¹¹B₁¹⁴N₁¹⁶O₁₂¹⁰¹Ru₄ 795).

Crystal Structure Determination.—Crystallographic data for compound **1** are collected in Table 1. Preliminary photographic characterization of a crystal mounted in a thin-walled capillary tube showed 2/*m* Laue symmetry, and the diffraction data contained the systematic absences for either of the monoclinic space groups *Cc* or *C2/c*. The centrosymmetric alternative was chosen initially and retained based on the chemically rational results of the refinement. A semi-empirical correction for absorption was applied to the data. The Ru atoms were located by direct methods. All non-hydrogen atoms were refined with anisotropic thermal parameters. All hydrogen atoms were located and isotropically refined. All computations used the SHELXTL-PC software.¹⁹ Atomic coordinates are given in Table 2.

Additional material available from the Cambridge Crystallographic Data Centre comprises H-atom coordinates, thermal parameters and remaining bond lengths and angles.

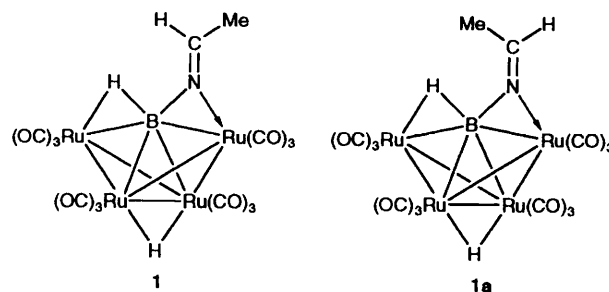
Molecular Orbital Calculations.—Fenske-Hall calculations²⁰ were carried out on compound **1** (with coordinates determined from the crystal structure) in terms of orbital interactions between the fragments {Ru₄H(CO)₁₂BH}⁻ and {MeHC=N}⁺. The calculations employed single-ζ Slater functions for the 1s and 2s orbitals of B, C, N and O. Exponents were obtained by curve fitting the double-ζ functions of Clementi²¹ while maintaining orthogonal functions. Double-ζ functions were used directly for the 2p orbitals. An exponent of 1.16 was used for H. The Ru atoms²² were augmented by 5s and 5p functions with exponents of 2.20.

Results and Discussion

Synthesis and Crystal Structure of Compound 1.—The triruthenaborane [Ru₃(CO)₉BH₃] readily undergoes spon-

Table 2 Atomic coordinates (× 10⁴) for compound **1**

Atom	<i>x</i>	<i>y</i>	<i>z</i>
Ru(1)	716(1)	1677(1)	4661(1)
Ru(2)	1284(1)	3621(1)	4545(1)
Ru(3)	1503(1)	858(1)	5465(1)
Ru(4)	1827(1)	3363(1)	6594(1)
N	879(1)	2620(4)	6103(3)
B	1245(1)	2718(5)	5983(3)
O(1)	604(1)	430(5)	2563(3)
O(2)	382(1)	-1035(4)	5215(4)
O(3)	0(1)	3484(6)	3723(4)
O(4)	782(2)	6023(5)	4774(4)
O(5)	912(1)	3466(5)	2196(3)
O(6)	1903(1)	5643(5)	4415(4)
O(7)	1417(2)	-713(5)	7264(4)
O(8)	1263(2)	-1649(5)	3968(4)
O(9)	2334(1)	-21(5)	6011(4)
O(10)	2268(1)	1888(5)	8617(3)
O(11)	2532(1)	3412(5)	5959(4)
O(12)	1926(2)	6499(4)	7224(4)
C(1)	659(2)	909(6)	3354(4)
C(2)	505(1)	-34(6)	5029(4)
C(3)	265(2)	2809(6)	4069(5)
C(4)	977(2)	5143(6)	4693(4)
C(5)	1037(2)	3481(5)	3066(4)
C(6)	1687(2)	4829(6)	4491(4)
C(7)	1451(2)	-149(6)	6593(4)
C(8)	1341(2)	-690(6)	4512(4)
C(9)	2030(1)	366(6)	5818(4)
C(10)	2116(2)	2469(6)	7876(4)
C(11)	2266(1)	3373(5)	6151(4)
C(12)	1898(2)	5314(6)	6997(4)
C(13)	755(2)	3026(5)	6797(4)
C(14)	357(2)	2881(8)	6743(7)



taneous cluster expansion to form [Ru₄H(CO)₁₂BH₂] and [Ru₆H(CO)₁₇B]. Increased product yields are obtained under conditions of photolysis.²³ Heterometallic fragments containing metals from Groups 6,²⁴ 8²³ and 9²⁵ have been successfully introduced to give products with Ru₃M frameworks. Our studies of the reactions of Group 6 metal complexes with [Ru₃(CO)₉BH₅] have included the use of [{M(η⁵-C₅H₅)(CO)₃]₂] (M = Mo or W)²⁴ and [M(CO)_{6-x}(MeCN)_x] (M = Cr, Mo or W; *x* = 1 or 2). In the latter case, the acetonitrile derivative is known to be an active source of the Group 6 metal carbonyl fragments,^{26,27} but the photolysis of [Ru₃(CO)₉BH₅] with [M(CO)_{6-x}(MeCN)_x] (M = Cr, Mo or W; *x* = 1 or 2), prepared *in situ*, failed to yield heterometallic products. Instead, the course of the reaction led to [Ru₄H(CO)₁₂BH₂] (a pathway that we have already observed),²³ and to a new boron-containing species, compound **1**. The isotopic distribution of the parent envelope in the mass spectrum of **1** suggested that this product possessed an Ru₄ framework. A second isomer of the product, **1a**, was also separated, although **1** was greatly favoured over **1a**. The spectroscopic and mass spectrometric data for **1a** were very similar to those of **1**.

A crystal of compound **1** suitable for X-ray diffraction was grown from CH_2Cl_2 layered with hexane. The molecular structure is shown in Fig. 1 and selected bond distances and angles are given in Table 3. Compound **1** contains an Ru_4 -butterfly skeleton with a boron atom in a semi-interstitial position and the structure is clearly related to that of $[\text{Ru}_4\text{H}(\text{CO})_{12}\text{BH}_2]$.¹⁷ The most interesting feature is the bridging amido group, which resembles the edge-bridging $\text{P}=\text{CBu}^+(\text{OSiMe}_3)$ group in the phosphaborane $\text{B}_5\text{H}_8\{\mu\text{-P}=\text{CBu}^+(\text{OSiMe}_3)\}$.²⁸ In compound **1**, the edge $\text{Ru}(1)\text{-B}$ is bridged by the nitrogen atom of the amido unit and suffers some elongation as a consequence; for the two wing-tip interactions, $\text{Ru}(1)\text{-B}$ 2.377(4) and $\text{Ru}(4)\text{-B}$ 2.130(5) Å, as compared to values of 2.111(6) and 2.106(6) Å in $[\text{Ru}_4\text{H}(\text{CO})_{12}\text{BH}_2]$.¹⁷ The hinge ruthenium-boron distances in **1** are comparable to those in $[\text{Ru}_4\text{H}(\text{CO})_{12}\text{BH}_2]$.¹⁷ Compared to $[\text{Ru}_4\text{H}(\text{CO})_{12}\text{BH}_2]$, the boron atom in **1** is drawn out of the butterfly framework; the height of the boron atom above the $\text{Ru}(1)\text{-Ru}(4)$ axis is 0.55 Å as compared to a value of 0.39 Å in $[\text{Ru}_4\text{H}(\text{CO})_{12}\text{BH}_2]$.^{*} The dihedral angle of the Ru_4 framework opens up from 118° in $[\text{Ru}_4\text{H}(\text{CO})_{12}\text{BH}_2]$ ¹⁷ to 124.5° in **1**. Each ruthenium atom in **1** also bears three terminal carbonyl ligands which are unexceptional.

The hydrogen atoms in compound **1** were located crystallographically. The ^1H NMR spectrum is instructive and also aids in the assignment of the hydrogen atoms. The ^1H NMR spectrum (CDCl_3) exhibits a broad resonance at $\delta -8.0$ and a sharp singlet at $\delta -20.44$. These signals correspond respectively to the presence of Ru-H-B and Ru-H-Ru bridging hydrogen atoms, and are close to the values observed for the $\text{Ru}_{\text{wing-tip}}\text{-H-B}$ ($\delta -8.4$, CDCl_3) and $\text{Ru}_{\text{hinge}}\text{-H-Ru}_{\text{hinge}}$ ($\delta -21.18$, CDCl_3) bridging hydrogen atoms in $[\text{Ru}_4\text{H}(\text{CO})_{12}\text{BH}_2]$.¹⁶ {Note that the values are also similar for $[\text{Ru}_4\text{H}(\text{CO})_{12}\text{BH}_2]$ in $(\text{CD}_3)_2\text{CO}$.¹⁷} The carbonyl orientations around atoms $\text{Ru}(2)$, $\text{Ru}(3)$ and $\text{Ru}(4)$ (Fig. 1) support the placement of one bridging hydrogen atom along each of the edges $\text{Ru}(4)\text{-B}$ and $\text{Ru}(2)\text{-Ru}(3)$ as shown in Fig. 1. The ^1H NMR spectrum also supports the presence of an amido functionality: a doublet at $\delta +2.3$ ($J_{\text{HH}} 4.8$ Hz) and a quartet at $\delta +8.8$ ($J_{\text{HH}} 5.0$ Hz) exhibit relative integrals of 3:1. These signals correspond to the methyl group involving $\text{C}(14)$ and the hydrogen atom directly attached to $\text{C}(13)$. The $\text{C}(13)\text{-N}$ distance is 1.274(7) Å, consistent with $\text{C}=\text{N}$ double bond character.

In the light of the crystallographic data for compound **1**, we propose that isomer **1a** differs only in the orientation of the $\text{N}=\text{CHMe}$ group with respect to the Ru_4B framework.

The bonding mode of the $\text{N}=\text{CHMe}$ group is of interest. A cluster featuring a butterfly skeleton is characterized by having 62 valence electrons. In $[\text{Ru}_4\text{H}(\text{CO})_{12}\text{BH}_2]$ this is achieved by allowing the boron atom to contribute all three of its valence electrons to cluster bonding; each hydrogen atom provides one electron and each $\text{Ru}(\text{CO})_3$ unit provides 14. This scheme was first detailed for the analogous ferraborane cluster $[\text{Fe}_4\text{H}(\text{CO})_{12}\text{BH}_2]$ ²⁹ and is also appropriate for $[\text{Os}_4\text{H}(\text{CO})_{12}\text{BH}_2]$.³⁰ The bridging mode of the amido group in **1** is consistent with the nitrogen atom acting as a three-electron donor overall. In order for compound **1** to be consistent with a 62-electron count, a localized two-centre two-electron B-N bond should be assigned. This leaves the boron atom to contribute two electrons to the cluster, and the nitrogen atom formally forms a co-ordinate bond to $\text{Ru}(1)$. This bonding scenario has been tested at the Fenske-Hall level and the results are discussed below. The bonding mode of the amido group in **1** may be compared with that of the $\text{C}(\text{Ph})=\text{CHPh}$ group in $[\text{Ru}_3\text{WH}(\eta^5\text{-C}_5\text{H}_5)(\text{CO})_{11}\text{B}\{\text{C}(\text{Ph})=\text{CHPh}\}]$ **2**.¹³ This cluster also retains a butterfly geometry and the required 62 valence

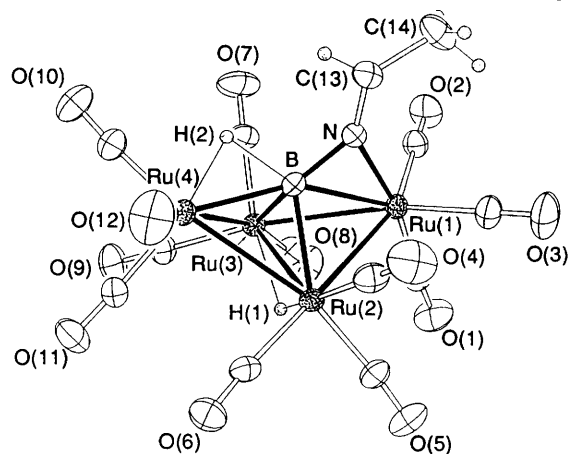
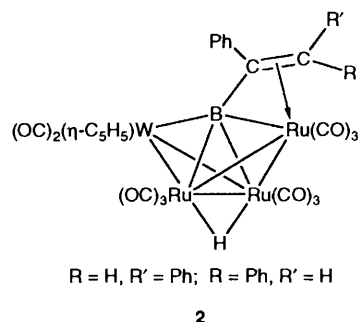


Fig. 1 Molecular structure of $[\text{Ru}_4\text{H}(\text{CO})_{12}\text{BH}(\mu\text{-NCHMe})]$ **1**

Table 3 Selected bond distances (Å) and angles ($^\circ$) for compound **1**

$\text{Ru}(1)\text{-Ru}(2)$	2.853(1)	$\text{Ru}(4)\text{-B}$	2.130(5)
$\text{Ru}(1)\text{-Ru}(3)$	2.868(1)	B-N	1.450(7)
$\text{Ru}(2)\text{-Ru}(3)$	2.867(1)	$\text{N-C}(13)$	1.274(7)
$\text{Ru}(2)\text{-Ru}(4)$	2.856(1)	$\text{C}(13)\text{-C}(14)$	1.481(10)
$\text{Ru}(3)\text{-Ru}(4)$	2.837(1)	$\text{Ru}(2)\text{-H}(1)$	1.91(5)
$\text{Ru}(1)\text{-B}$	2.377(4)	$\text{Ru}(3)\text{-H}(1)$	1.80(5)
$\text{Ru}(1)\text{-N}$	2.072(4)	$\text{Ru}(4)\text{-H}(2)$	1.61(6)
$\text{Ru}(2)\text{-B}$	2.225(5)	$\text{B}(1)\text{-H}(2)$	1.69(7)
$\text{Ru}(3)\text{-B}$	2.233(5)		
Ru-Ru-Ru	all 60.0 ± 0.5	$\text{Ru}(1)\text{-B-N}$	59.9(2)
$\text{Ru}(1)\text{-B-Ru}(2)$	76.6(1)	$\text{Ru}(2)\text{-B-N}$	120.1(3)
$\text{Ru}(1)\text{-B-Ru}(3)$	76.9(1)	$\text{Ru}(3)\text{-B-N}$	122.0(3)
$\text{Ru}(1)\text{-B-Ru}(4)$	151.4(3)	$\text{Ru}(4)\text{-B-N}$	148.7(3)
$\text{Ru}(2)\text{-B-Ru}(3)$	80.0(2)	$\text{Ru}(1)\text{-N-C}(13)$	143.2(3)
$\text{Ru}(2)\text{-B-Ru}(4)$	81.9(2)	$\text{B-N-C}(13)$	133.8(4)
$\text{Ru}(3)\text{-B-Ru}(4)$	81.1(2)	$\text{N-C}(13)\text{-C}(14)$	125.1(5)
$\text{Ru}(1)\text{-N-B}$	82.9(3)		



electron count can be achieved if one assigns a localized B-C bond and a two-electron π interaction from the alkene to a wing-tip ruthenium atom. In contrast, however, in $[\text{Ru}_4\text{H}(\text{CO})_{12}\text{BH}\{\text{C}(\text{Ph})=\text{CHPh}\}]$ the boron continues to use all three of its valence electrons for cluster bonding and a 64-electron spiked triangle (or a butterfly with one edge broken) results.^{12,13}

Electronic Structure of Compound 1.—The electronic structure of cluster **1** has been examined by using the Fenske-Hall quantum chemical method. The bonding has been considered in terms of the interactions between the two fragments $\{\text{Ru}_4\text{H}(\text{CO})_{12}\text{BH}\}^-$ and $\{\text{MeHC}=\text{N}\}^+$; for the calculations, each of these fragments is given the same geometry as is experimentally observed in complex **1**. The frontier molecular orbitals (MOs) of the $\{\text{MeHC}=\text{N}\}^+$ unit are shown schematically in

* Value calculated from the atomic coordinates of $[\text{Ru}_4\text{H}(\text{CO})_{12}\text{BH}_2]$ given in ref. 17.

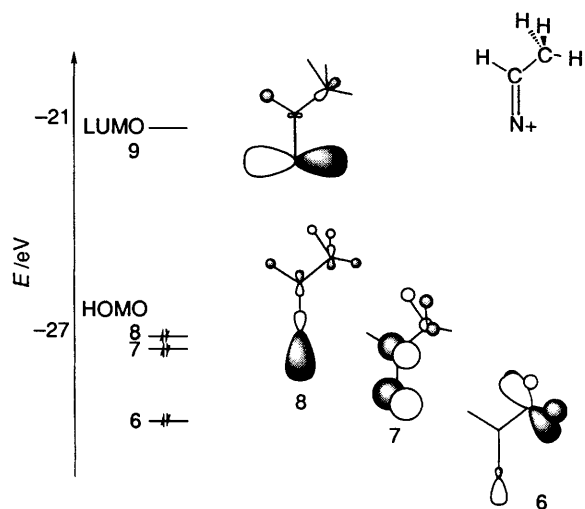


Fig. 2 Frontier molecular orbitals of the $\{\text{MeHC}=\text{N}\}^+$ fragment; $\text{eV} \approx 1.60 \times 10^{-19} \text{ J}$

Fig. 2; the next lowest lying unoccupied MO (the $\text{C}=\text{N} \pi^*$ orbital, MO 10) is at -10.5 eV . Orbital 8 [the highest occupied molecular orbital (HOMO)] is centred on the nitrogen atom with 60% 2p and 13% 2s character. Molecular orbital 6 also possesses nitrogen 2p (96%) and 2s (5%) character but is mainly methyl-bonding in character. The lowest unoccupied molecular orbital (LUMO) (MO 9) has 81% nitrogen character (pure 2p). When one considers the relative positions of the two fragments as they come together to form **1**, MO 9 is directed parallel to the $\text{Ru}_{\text{wing-tip}} \cdots \text{Ru}_{\text{wing-tip}}$ axis of the $\{\text{Ru}_4\text{H}(\text{CO})_{12}\text{BH}\}^-$ fragment. Molecular orbital 7 of $\{\text{MeHC}=\text{N}\}^+$ is primarily a $\text{C}=\text{N} \pi$ -bonding orbital (53% N 2p and 20% C 2p) and the directionality of this MO coincides with the $\text{Ru}_{\text{hinge}} \cdots \text{Ru}_{\text{hinge}}$ axis of the $\{\text{Ru}_4\text{H}(\text{CO})_{12}\text{BH}\}^-$ fragment.

The electronic structure of the butterfly cluster $[\text{Fe}_4\text{H}(\text{CO})_{12}\text{BH}]^-$ has been previously described²⁷ as has that of $[\text{Fe}_4(\text{CO})_{12}\text{BH}_2]^-$,³¹ and details of the bonding in the analogous tetraruthenium cluster unit $\{\text{Ru}_4\text{H}(\text{CO})_{12}\text{BH}\}^-$ other than features required to understand the binding of the amido group are not discussed here. A point of significance however is the consequence of raising the boron atom out of the butterfly framework. In a study of the model compound $[\text{HB}_4\text{H}_4\text{C}]^-$,³² we illustrated that raising the central carbon atom above the $\text{B}_{\text{wing-tip}} \cdots \text{B}_{\text{wing-tip}}$ axis of the B_4 -butterfly framework exposed a high lying occupied MO with carbon sp character; protonation of this model $[\text{HB}_4\text{H}_4\text{C}]^-$ anion led to the formation of a localized, terminal C–H bond. Forcing the carbon atom down to be colinear with the two wing-tip boron atoms (*i.e.* modelling a carbide) exposed a HOMO which was of $\text{B}_{\text{wing-tip}}\text{--C}$ bonding character. Protonation of this model led to the formation of a bridging B–H–C interaction. These model situations are extreme but illustrate that in the M_4 -butterfly systems, the structural observation of a semi-interstitial atom being ‘pulled out’ from its M_4 cavity is concomitant with the formation of a localized bond to this atom. The experimentally determined structure of **1** shows that the boron atom is 0.16 \AA further above the $\text{Ru}_{\text{wing-tip}} \cdots \text{Ru}_{\text{wing-tip}}$ axis than in $[\text{Ru}_4\text{H}(\text{CO})_{12}\text{BH}_2]$. Of the frontier MOs of the $\{\text{Ru}_4\text{H}(\text{CO})_{12}\text{BH}\}^-$ fragment studied here, five have a significant degree of boron character: MO 81 (unoccupied), MO 79 (HOMO) and MOs 77, 76 and 75. The lowest lying of these MOs exhibit boron 2p character with the lobe directed parallel to the $\text{Ru}_{\text{hinge}} \cdots \text{Ru}_{\text{hinge}}$ axis. Molecular orbitals 77 and 79 (Fig. 3) both have Ru–B bonding character although, in MO 77, the 2p orbital on the boron atom is directed outwards from the butterfly framework rather than towards the orbital lobe of the wing-tip ruthenium atom. Molecular orbital 81 is antibonding with respect to the $\text{Ru}_{\text{wing-tip}}\text{--B}$ interactions (Fig. 3).

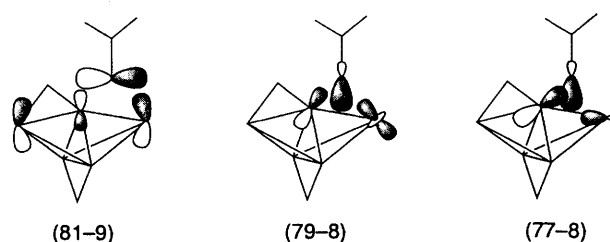


Fig. 3 Schematic representations of the three major $\{\text{Ru}_4\text{H}(\text{CO})_{12}\text{BH}\}^- \cdots \{\text{MeHC}=\text{N}\}^+$ inter-fragment orbital interactions which together contribute 78% of the total inter-fragment bonding

The $\{\text{Ru}_4\text{H}(\text{CO})_{12}\text{BH}\}^- \cdots \{\text{MeHC}=\text{N}\}^+$ inter-fragment Mulliken overlap populations are given in Table 4 and the contribution that each inter-fragment interaction makes to the total overlap population is highlighted. It may be seen that 78% of the total is bound up in three $\{\text{Ru}_4\text{H}(\text{CO})_{12}\text{BH}\}^- \cdots \{\text{MeHC}=\text{N}\}^+$ orbital interactions, namely (81–9), (79–8) and (77–8). These three orbital interactions are schematically represented in Fig. 3. Each of the combinations (81–9), (79–8) and (77–8) generates Ru–N and B–N bonding interactions, although (77–8) lies in favour of overlap along the B–N vector due to the directionality of the 2p lobe on the boron atom in fragment MO 77.

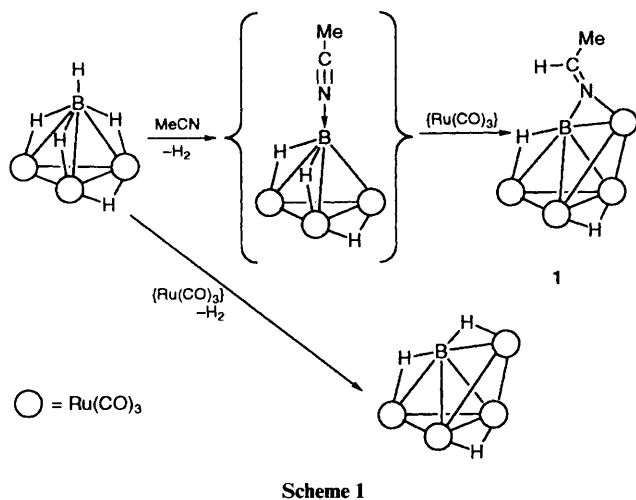
An analysis of the character of the molecular orbitals of compound **1** in terms of percentage contributions from the orbitals of the $\{\text{Ru}_4\text{H}(\text{CO})_{12}\text{BH}\}^-$ and $\{\text{MeHC}=\text{N}\}^+$ fragments indicates that the three principal interactions (81–9), (79–8) and (77–8) are localized in three MOs in **1**. Molecular orbital 68 of **1** exhibits both the (79–8) and (77–8) interactions, and (81–9) is contained in MOs 70 and 71 of **1**; (the HOMO of **1** is MO 87). This degree of localization is consistent with the notion that the boron atom is involved in a localized B–N bonding interaction which lies externally to the cluster core. The results of the Fenske–Hall treatment support the conclusions drawn from a consideration of the bonding in terms of the cluster valence electron count.

Reaction Pathway.—The formation of compound **1** in a reaction mixture that contains $[\text{Ru}_3(\text{CO})_9\text{BH}_5]$, $[\text{M}(\text{CO})_6]$ ($\text{M} = \text{Cr}, \text{Mo}$ or W), Me_3NO and MeCN was not anticipated. Since we had previously observed coupling of alkynes with the boron atom in $[\text{Ru}_4\text{H}(\text{CO})_{12}\text{BH}_2]$ and $[\text{Ru}_3\text{WH}(\eta^5\text{-C}_5\text{H}_5)(\text{CO})_{11}\text{BH}]$,^{12–14} we initially thought that **1** was formed from a reaction between MeCN and $[\text{Ru}_4\text{H}(\text{CO})_{12}\text{BH}_2]$. The latter is known to form during the photolysis of $[\text{Ru}_3(\text{CO})_9\text{BH}_5]$,²³ and was indeed observed as a product in the reaction described here (see Experimental section). However, attempts to obtain **1** by the direct reaction of MeCN and $[\text{Ru}_4\text{H}(\text{CO})_{12}\text{BH}_2]$ under conditions of photolysis led only to the formation of $[\text{Ru}_6\text{H}(\text{CO})_{17}\text{B}]$ ^{23,33} and unidentified products of decomposition. Attempts to prepare it by photolysing $[\text{Ru}_3(\text{CO})_9\text{BH}_5]$ in MeCN also failed. The presence of the Group 6 metal carbonyl and Me_3NO proved to be an important feature. However, an analogous reaction in which this species was replaced by the Group 7 metal complex $[\text{Mn}(\text{CO})_5(\text{MeCN})]^+$ ³⁴ also failed to produce **1**. Significantly though, the formation of **1** under the conditions described in this work is certainly a reproducible reaction and leads us to suggest a possible pathway.

In iron and ruthenium chemistry, the trimetal species $[\text{Fe}_3(\text{CO})_9\text{BH}_5]$ ^{35,36} and $[\text{Ru}_3(\text{CO})_9\text{BH}_5]$ ¹⁵ have been isolated and shown to exhibit both M–H–B and M–H–M interactions. On the other hand, the osmium analogue of these clusters has not been reported although Shore and co-workers^{7,11} have prepared and characterized related compounds of the type $[\text{Os}_3\text{H}_3(\text{CO})_9\text{B}(\text{L})]$ where L is a two-electron donor such as CO ^{7,11} or PMe_3 .¹¹ Fehlner and co-workers have recently reported the related system $[\text{Fe}_3\text{H}(\text{CO})_9\text{B}(\text{CO})]^{2-}$.³⁷ With

Table 4 Inter-fragment Mulliken overlap populations for the interaction of $\{\text{Ru}_4\text{H}(\text{CO})_{12}\text{BH}\}^-$ and $\{\text{MeHC}=\text{N}\}^+$ to form compound **1**. The percentages given are the contributions of the individual overlaps to the total Mulliken overlap population

Fragment MOs for $\{\text{Ru}_4\text{H}(\text{CO})_{12}\text{BH}\}^-$	Fragment MOs for $\{\text{MeHC}=\text{N}\}^+$			
	6	7	8 (HOMO)	9 (LUMO)
81				0.112 (31%)
80 (LUMO)				
79 (HOMO)	0.021 (6%)		0.108 (30%)	
78				0.022 (6%)
77	0.013 (4%)		0.060 (17%)	
64			0.012 (3%)	
61			0.012 (3%)	



these and our experimental observations in mind, we suggest that a possible pathway from $[\text{Ru}_3(\text{CO})_9\text{BH}_5]$ to **1** may involve an intermediate $\{\text{Ru}_3(\text{CO})_9\text{BH}_3(\text{NCMe})\}$ as illustrated in Scheme 1. The intermediate could have one of several arrangements of the three cluster hydrogen atoms. Note that in $[\text{Os}_3\text{H}_3(\text{CO})_9\text{B}(\text{CO})]$ ^{7,11} and $[\text{Os}_3\text{H}_3(\text{CO})_9\text{B}(\text{PMe}_3)]$,⁷ all three hydrogen atoms bridge Os–Os edges. As it is formed, we propose that $\{\text{Ru}_3(\text{CO})_9\text{BH}_3(\text{NCMe})\}$ undergoes cluster expansion to give **1**; this would involve the transfer of one cluster-bonded hydrogen atom to the acetonitrile ligand, converting it into an amido residue. We suggest that this expansion competes with the direct expansion of $[\text{Ru}_3(\text{CO})_9\text{BH}_5]$ to $[\text{Ru}_4\text{H}(\text{CO})_{12}\text{BH}_2]$ (Scheme 1).²³ We have been unable to delineate the role of the Group 6 metal in the formation of compound **1**. However, under the reaction conditions, decarbonylation of $[\text{M}(\text{CO})_6]$ should provide a coordinatively unsaturated Group 6 species that may be the active species in the reaction. Group 6-containing products have not been isolated from the product separation and we must conclude that they lie in the insoluble residue on the TLC plate.

Acknowledgements

Acknowledgements are made to the donors of the Petroleum Research Fund, administered by the American Chemical Society for support of this work (grants #25533-AC3 and #22771-AC3), to the SERC for studentships (to J. R. G. and J. S. H.) and to the National Science Foundation for a grant (CHE 9007852) towards the purchase of a diffractometer at the University of Delaware.

References

- 1 C. E. Housecroft, *Polyhedron*, 1987, **6**, 1935.
- 2 T. P. Fehlner, *New J. Chem.*, 1988, **12**, 307.
- 3 T. P. Fehlner, *Adv. Inorg. Chem.*, 1990, **35**, 199.
- 4 C. E. Housecroft, *Adv. Organomet. Chem.*, 1991, **33**, 1.

- 5 C. E. Housecroft, in *Inorganometallic Chemistry (Modern Inorganic Chemistry)*, ed. T. P. Fehlner, Plenum, New York, 1992, ch. 3, p. 73.
- 6 See, for example, J. S. Bradley, *Adv. Organomet. Chem.*, 1983, **22**, 1; E. L. Muetterties, *Prog. Inorg. Chem.*, 1981, **28**, 203.
- 7 S. G. Shore, D.-Y. Jan, L.-Y. Hsu and W.-L. Hsu, *J. Am. Chem. Soc.*, 1983, **105**, 5923.
- 8 D.-Y. Jan, L.-Y. Hsu, D. P. Workman and S. G. Shore, *Organometallics*, 1987, **6**, 1984.
- 9 D.-Y. Jan and S. G. Shore, *Organometallics*, 1987, **6**, 428.
- 10 D. P. Workman, H.-B. Deng and S. G. Shore, *Angew. Chem., Int. Ed. Engl.*, 1990, **29**, 309.
- 11 D.-Y. Jan, D. P. Workman, L.-Y. Hsu, J. A. Krause and S. G. Shore, *Inorg. Chem.*, 1992, **31**, 5123.
- 12 A. K. Chipperfield, B. S. Haggerty, C. E. Housecroft and A. L. Rheingold, *J. Chem. Soc., Chem. Commun.*, 1990, 1174.
- 13 C. E. Housecroft, J. S. Humphrey, A. K. Keep, D. M. Matthews, N. J. Seed, B. S. Haggerty and A. L. Rheingold, *Organometallics*, 1992, **11**, 4048.
- 14 S. M. Draper, C. E. Housecroft, A. K. Keep, D. M. Matthews, B. S. Haggerty and A. L. Rheingold, *J. Organomet. Chem.*, 1991, **410**, C44.
- 15 A. K. Chipperfield and C. E. Housecroft, *J. Organomet. Chem.*, 1988, **349**, C17.
- 16 A. K. Chipperfield, C. E. Housecroft and A. L. Rheingold, *Organometallics*, 1990, **9**, 681.
- 17 F.-E. Hong, D. A. McCarthy, J. P. White, C. E. Cottrell and S. G. Shore, *Inorg. Chem.*, 1990, **29**, 2874.
- 18 C. R. Eady, B. F. G. Johnson and J. Lewis, *J. Chem. Soc., Dalton Trans.*, 1977, 477.
- 19 SHELXTL-PC software, G. Sheldrick, Siemens XRD, Madison, WI.
- 20 M. B. Hall and R. F. Fenske, *Inorg. Chem.*, 1972, **11**, 768.
- 21 E. Clementi, *J. Chem. Phys.*, 1964, **40**, 1944.
- 22 J. W. Richardson, M. J. Blackman and J. F. Ranochak, *J. Chem. Phys.*, 1973, **58**, 3010.
- 23 S. M. Draper, C. E. Housecroft, A. K. Keep, D. M. Matthews, X. Song and A. L. Rheingold, *J. Organomet. Chem.*, 1992, **423**, 241.
- 24 C. E. Housecroft, D. M. Matthews, A. L. Rheingold and X. Song, *J. Chem. Soc., Dalton Trans.*, 1992, 2855.
- 25 J. R. Galsworthy, C. E. Housecroft, R. Ostrander and A. L. Rheingold, *J. Chem. Soc., Dalton Trans.*, 1994, 69.
- 26 D. P. Tate, W. R. Knipple and J. M. Augl, *Inorg. Chem.*, 1962, **1**, 433.
- 27 G. J. Kubas, *Inorg. Chem.*, 1983, **22**, 692.
- 28 R. W. Miller, K. J. Donaghy and J. T. Spencer, *Organometallics*, 1991, **10**, 1161.
- 29 T. P. Fehlner, C. E. Housecroft, W. R. Scheidt and K. S. Wong, *Organometallics*, 1983, **2**, 825.
- 30 J.-H. Chung, D. Knoepfel, D. A. McCarthy, A. Columbie and S. G. Shore, *Inorg. Chem.*, 1993, **32**, 3391.
- 31 C. E. Housecroft and A. L. Rheingold, *Organometallics*, 1987, **6**, 1332.
- 32 C. E. Housecroft, *J. Organomet. Chem.*, 1984, **276**, 297.
- 33 F.-E. Hong, T. J. Coffy, D. A. McCarthy and S. G. Shore, *Inorg. Chem.*, 1989, **28**, 3284.
- 34 N. G. Connelly and L. F. Dahl, *Chem. Commun.*, 1970, 880.
- 35 J. C. Vites, C. Eigenbrot and T. P. Fehlner, *J. Am. Chem. Soc.*, 1984, **106**, 4633.
- 36 J. C. Vites, C. E. Housecroft, C. Eigenbrot, M. L. Buhl, G. J. Long and T. P. Fehlner, *J. Am. Chem. Soc.*, 1986, **108**, 3304.
- 37 L. E. Craswell, B. H. S. Thimmappa, A. L. Rheingold, R. Ostrander and T. P. Fehlner, *Organometallics*, 1994, **13**, 2153.